

Fundamental Limits of Optical Patterned Defect Metrology

Rick Silver

**National Institute of Standards and Technology
Surface and Microform Metrology Group**

B. Barnes

Tool Design and Data Acquisition

H. Zhou

Simulation and Analysis

Y. Sohn

193 nm Scatterfield Microscope

J. Qin

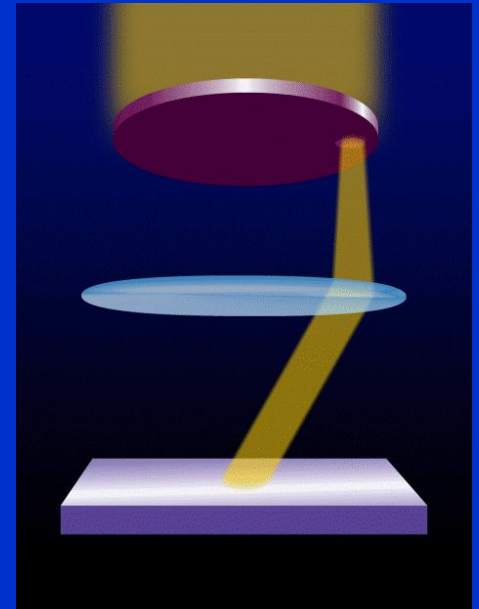
Tool Operation and Data Analysis

- **ITRS metrology roadmap shows defect inspection as red, without known solutions in just two years. We are working with the major manufacturers and suppliers to evaluate and develop new techniques to meet these needs.**
- **Need to measure large patterned areas for process control in manufacturing.**
- **There is a fundamental incompatibility between throughput and resolution.**
- **While there are metrology tools that provide adequate resolution, they have either inadequate throughput or no feasible cost basis.**

- **Optical methods offer unparalleled throughput with tremendous sensitivity. Dense arrayed and irregular features approaching 1/20th the wavelength can be measured.**
- **The arrayed and directional aspects of future device fabrication are well suited to engineered optical fields.**
- **Spatial frequency modulation of the illumination and collection fields can be tailored to enhance optical defect signals.**
- **Further gains can be achieved at shorter wavelengths.**
- **Don't need super-resolution to image each device, but need to image nm scale pattern and particle defects over large areas!**

Overview

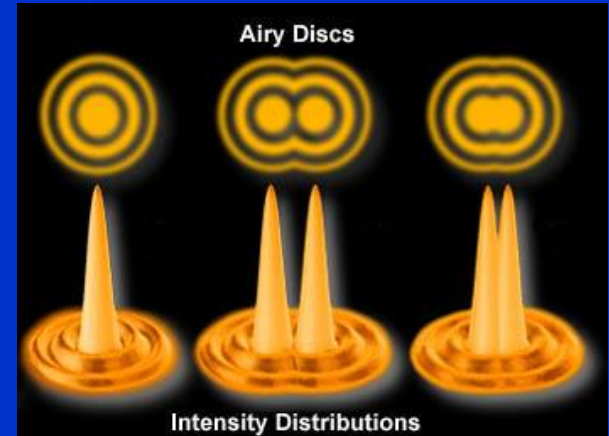
- **Scatterfield Optical Microscopy**
- **3-D simulations**
- **Comparisons using die-to-defect metrology**
- **$\lambda = 193$ nm defect detection experiments**
- **Interference-based defect metrology**
- **Future directions**



The Basis for Scatterfield Imaging

The perception of optical metrology limitations:

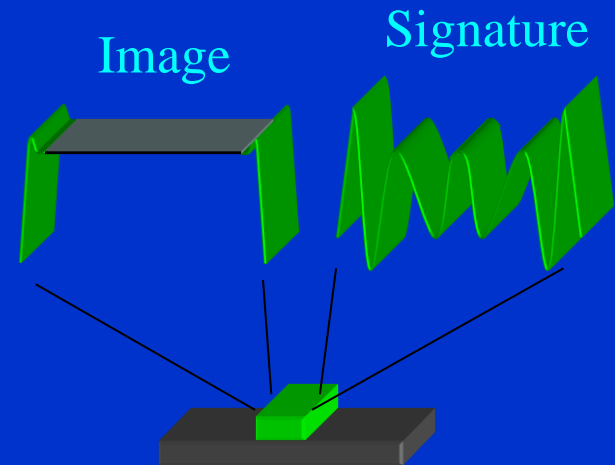
Beyond the Rayleigh criterion, what are the model-based optical metrology limits?



- Are we really limited by the wavelength?

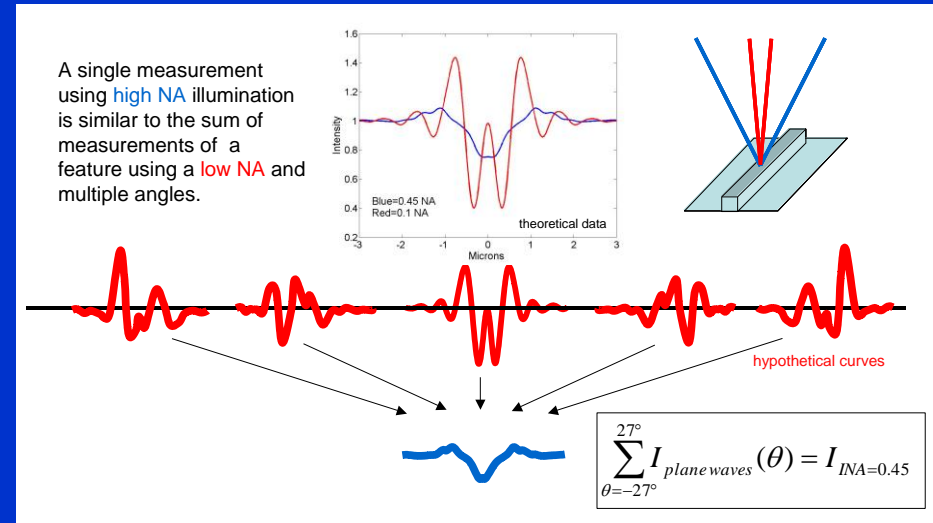


- Edge-based image analysis is not applicable
 - Go beyond standard edge algorithms and use the entire scattered field



Isolating the Optical Signal of Interest: Angle-resolved Scatterfield Imaging

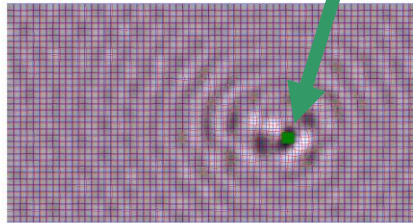
- When the intensities at each angle are summed, they result in a “blurred” or averaged signal. The valleys and hills in the profiles add to suppress optical image content.



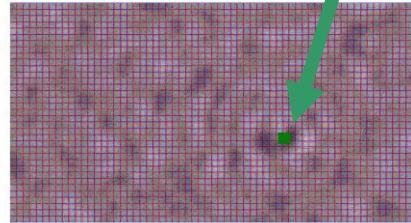
Initial detection

Continued detection

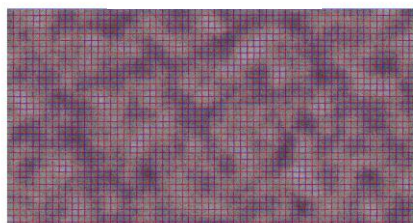
No noise



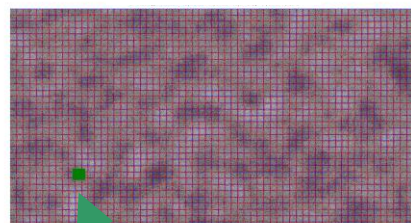
RMS noise = 0.5%



RMS noise = 1.25%



RMS noise = 2.0%

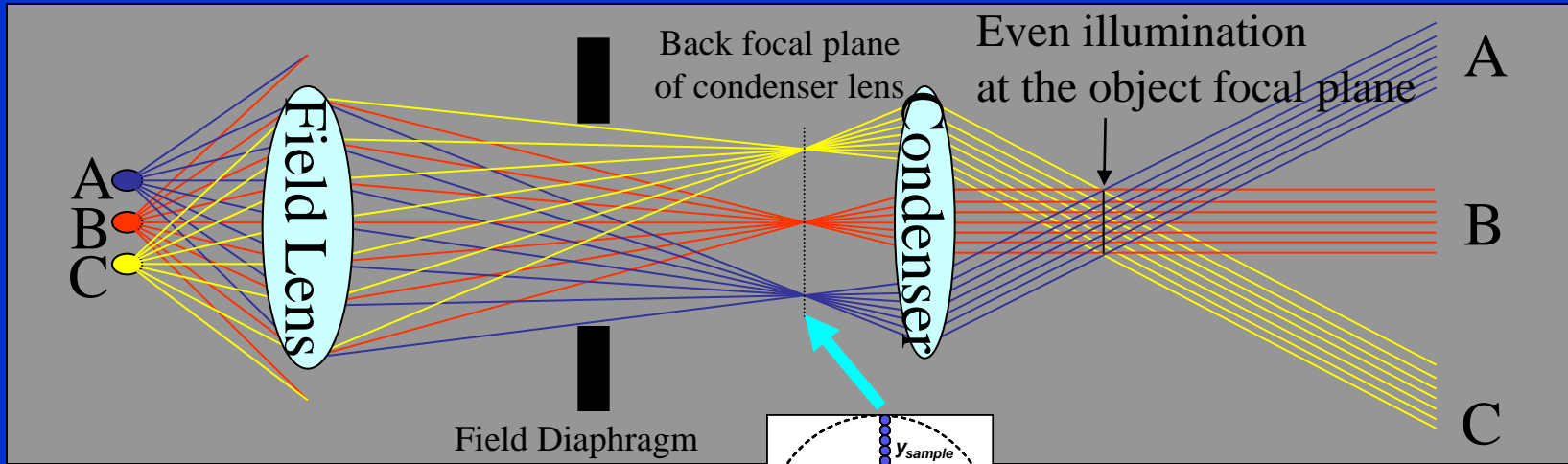


No defect detected

Noise causes
false positive

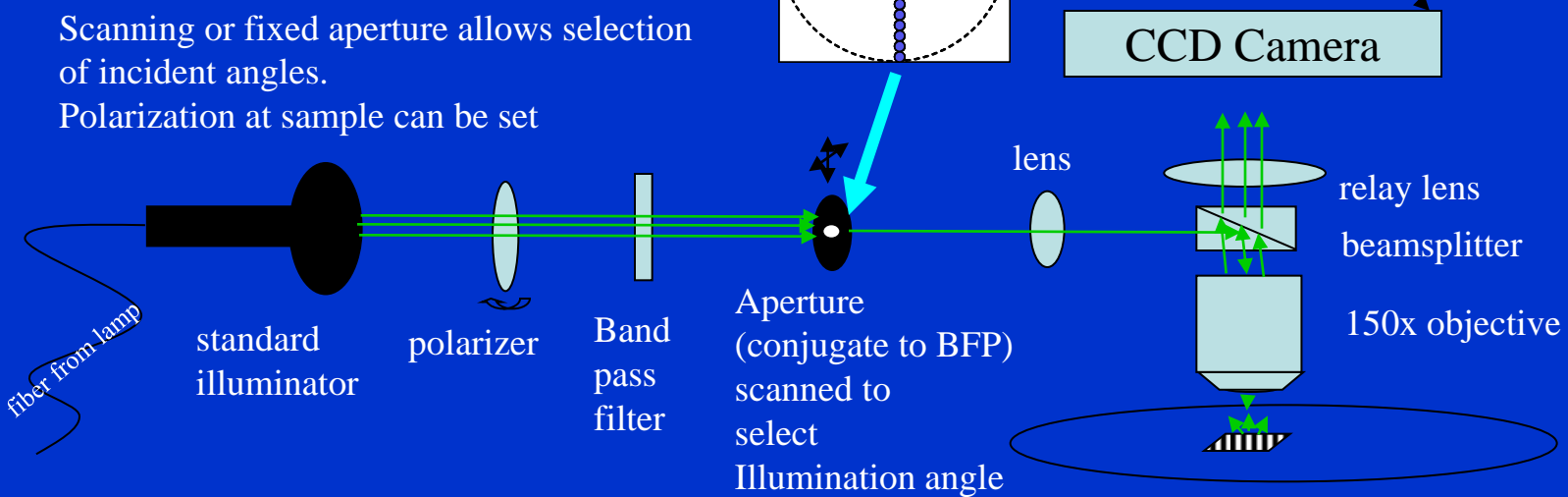
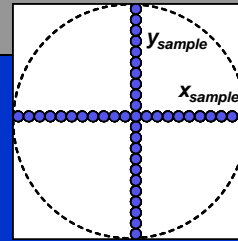
- Realistic noise models are a key to evaluating advanced defect detection.
- Sample noise is on the order of the defect signal.

The Scatterfield Optical Configuration



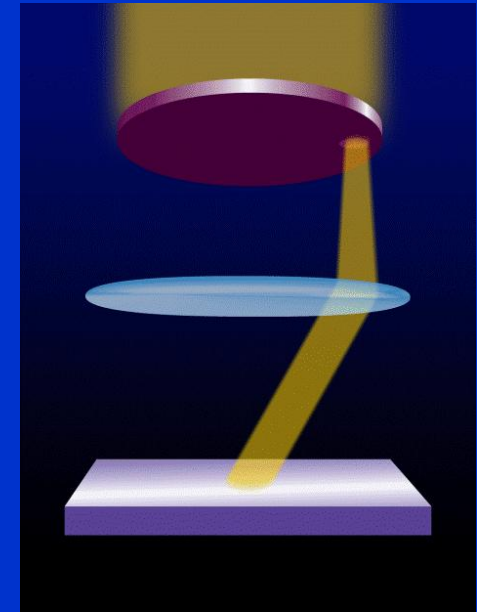
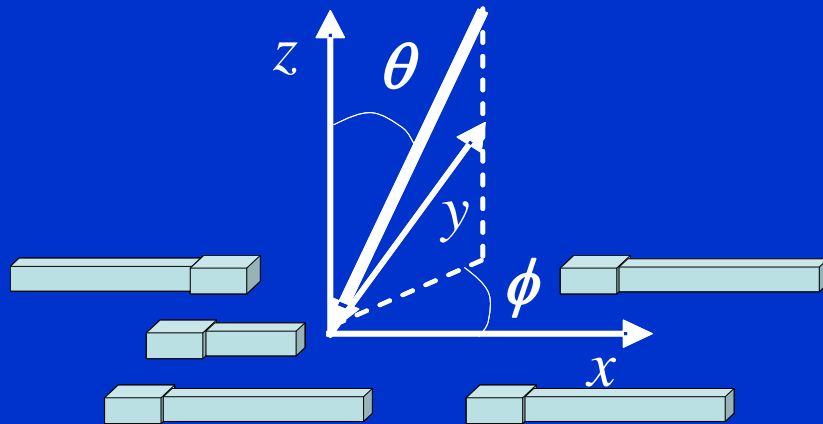
Köhler permits illumination engineering, such as off-axis illumination.

- Scanning or fixed aperture allows selection of incident angles.
- Polarization at sample can be set

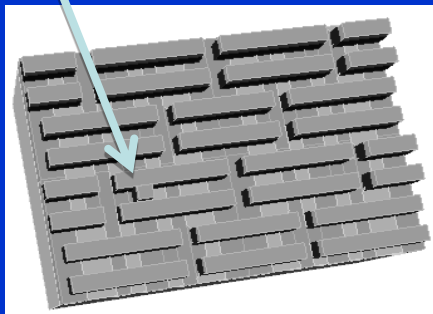


Here we use the scatterfield microscope in a high magnification angle-resolved mode. A spectroscopic version has also been demonstrated.

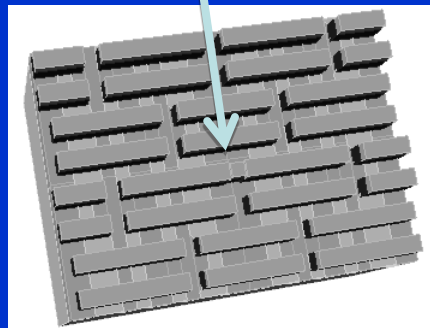
Source and Collection Optimization for Arrayed Patterns



line-to-line



end-to-end

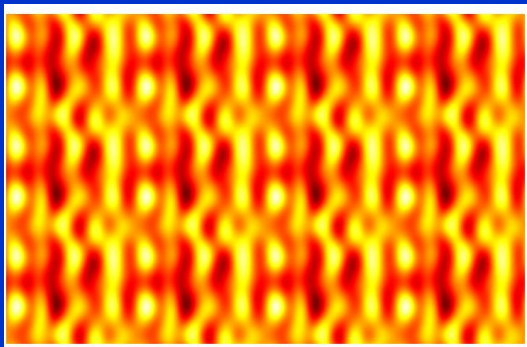


Optimizing optical defect inspection using:

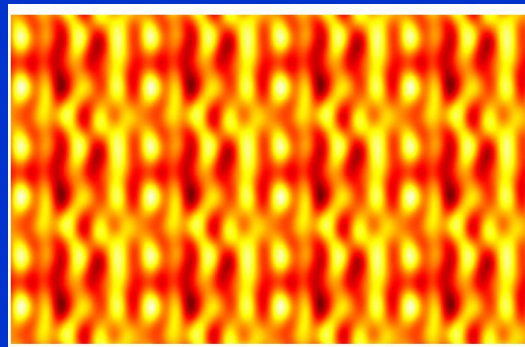
- wavelength
- Polarization
- spatial frequency
- control coherence

Simulations to Evaluate Trends and Develop the Tools

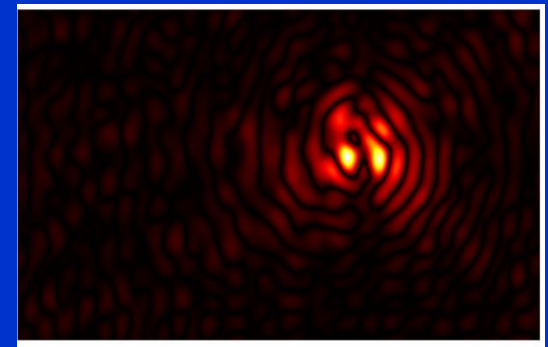
- **Three-dimensional simulations of structures are performed on defect from the 45 nm to defects below 10 nm.**
 - Finite-difference time-domain (FDTD)
 - Commercially available code
 - In-house code
 - Finite Element Method (FEM)
 - Commercially available code
 - Integral equation solver (in-house)
- **Results are subtracted for die-to-defect comparisons**



No Defect



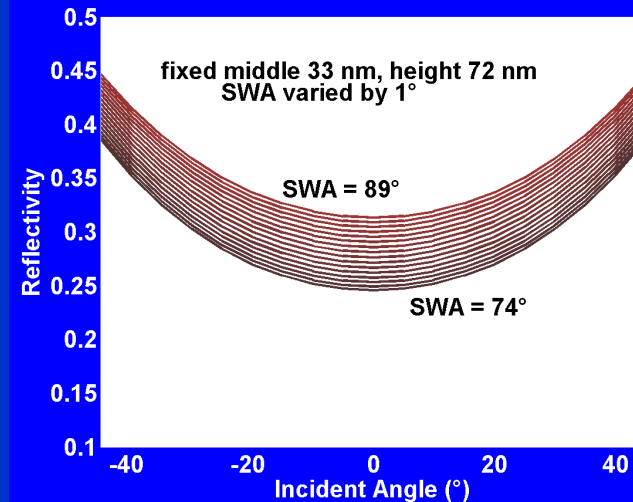
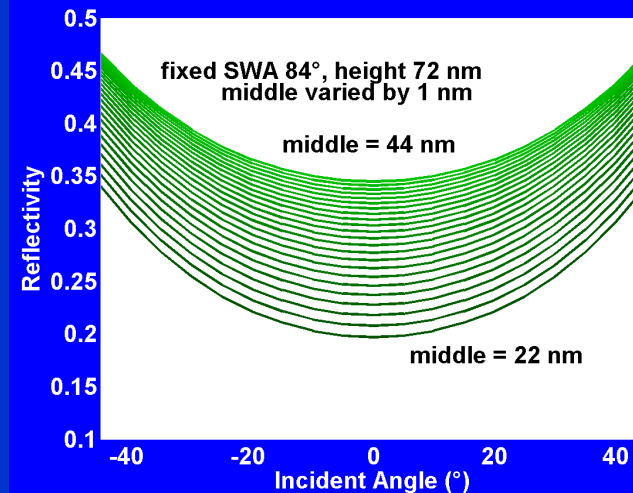
With Defect



Difference (absolute value)

High-magnification Platform Modeling Demonstration: Build a Simulation Library

- Parametric analysis:
 - Vary n and k
 - CD (top, mid, and bottom)
 - Height and pitch variation
 - Sidewall variation
 - LER
 - Footing and corner rounding
- Starting point of geometrical variations: AFM reference
 - X3D with full uncertainty analysis
- Several models used in comprehensive simulations
 - 3-Dim FDTD model
 - 3-Dim FEM model
 - 2 & 3-Dim RCWA



L50/P175
Parallel scan

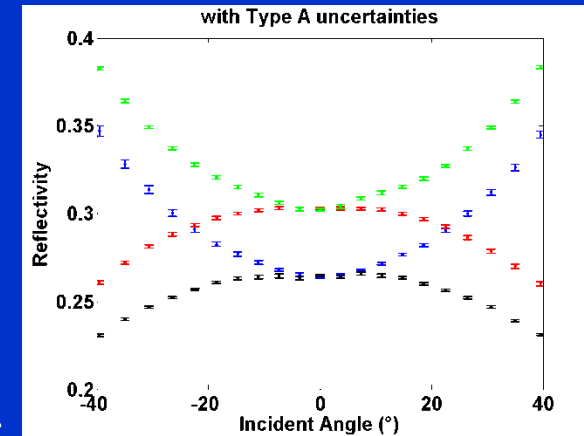
height:
68 nm to 76 nm
Middle width:
22 nm to 44 nm
SWA:
74 ° to 89°

For more complex stacks, we use fitted reflectivity curves from blanket materials.

Optical Measurements: Intensity versus Angle Scans

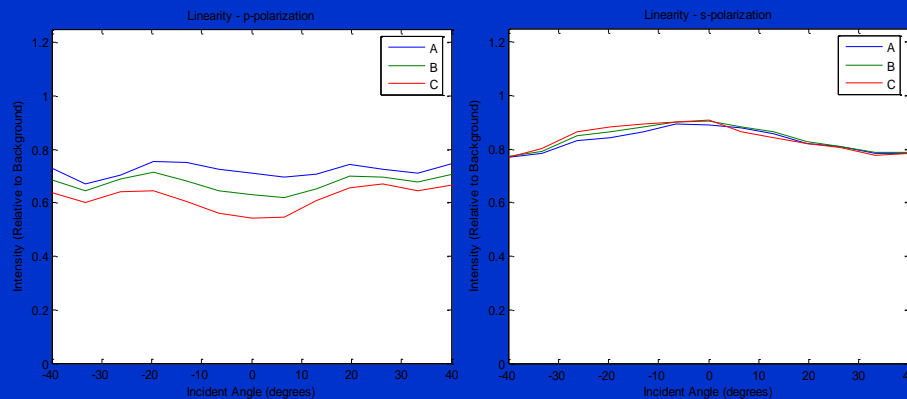
- One or more kernels are placed in an image and the total intensity for each kernel is integrated.
- The intensity is plotted as a function of angle.
- The intensity pattern may include only specular or higher order diffraction components.
- Similar to conventional scatterometry except high magnification imaging optics enable spatial resolution.

Full field signal normalization as a function of angle and polarization is required.

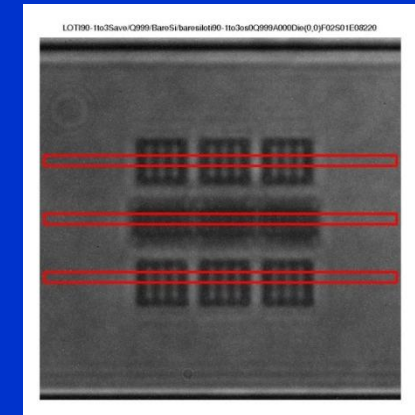


Angle-resolved intensity plot.

Full-field Parallel Scatterometry



Sub-arrays nominally 60 nm CD with 5 nm design increments.

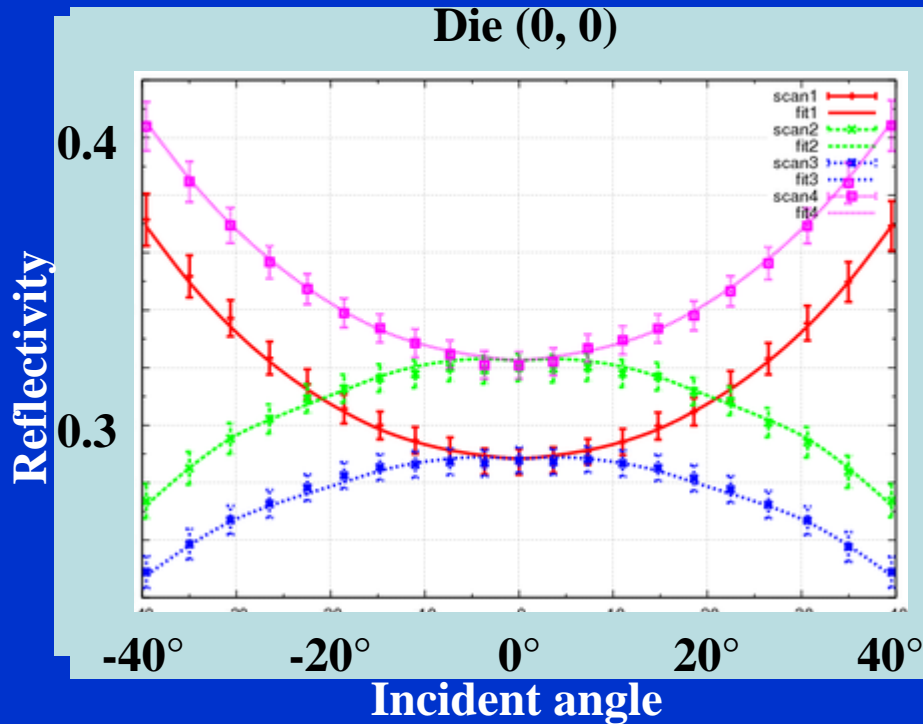


Linearity Target

We can perform either single, many parallel scatterometry measurements, or measure very small, embedded targets.

50 nm pillar array, 175 nm pitch at $\lambda=450$ nm

Die (0, 0)



OCD parameterization

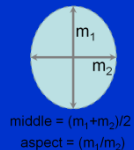
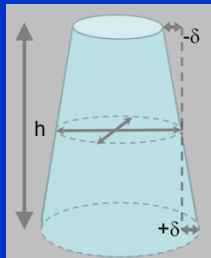
	a	σ_a
middle	45.27 nm	2.77 nm
δ	26.27 nm	6.61 nm
height	82.12 nm	5.99 nm
aspect	1.19	0.01

OCD with h_{AFM}

	a	σ_a
middle	49.01 nm	1.11 nm
δ	17.86 nm	3.35 nm
height	73.73 nm	1.10 nm
aspect	1.19	0.01

OCD with with δ_{AFM} and h_{AFM}

	a	σ_a
middle	48.91 nm	0.89 nm
δ	18.17 nm	2.63 nm
height	73.84 nm	1.78 nm
aspect	1.19	0.01



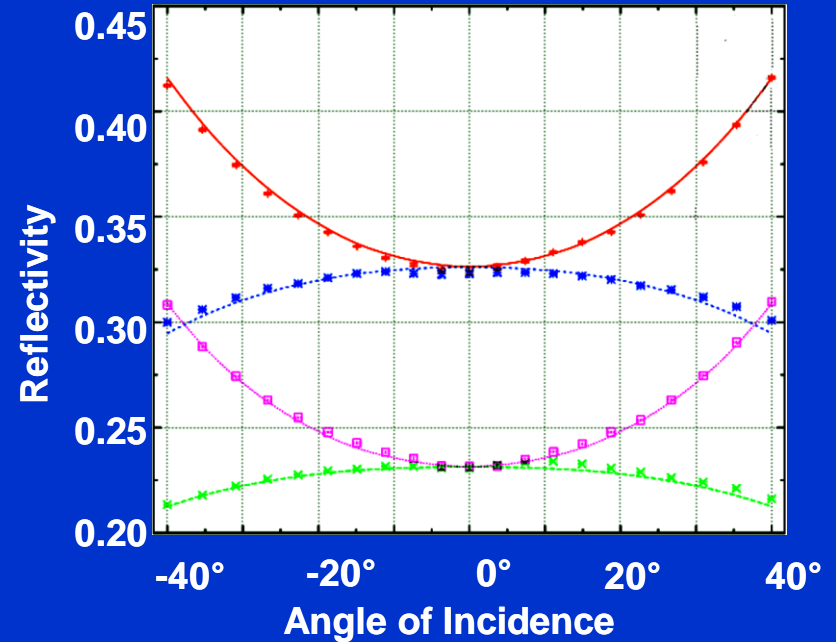
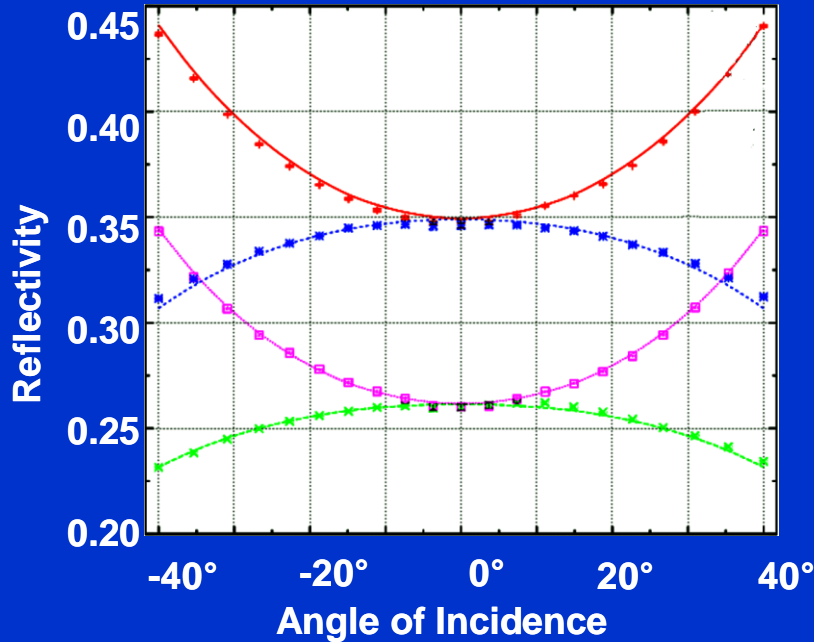
AFM values

middle = $55.3 \text{ nm} \pm 2.4 \text{ nm}$
 δ = $18.7 \text{ nm} \pm 4.2 \text{ nm}$
 height = $72.8 \text{ nm} \pm 2 \text{ nm}$

Lower right tables show measurements with new hybrid metrology approach embedding AFM.

Comparison with Reference Measurements for Nitride Stack

L50P175 Linewidth arrays. Values from various techniques shown.



	CD_{Top}	CD_{Mid}	CD_{Bot}	h	n
OCD	41	49	63	56	100%
AFM	38	45	50	55	
SAXS	43	53	62	54	
SEM	35	49	63		

	CD_{Top}	CD_{Mid}	CD_{Bot}	h	n
OCD	53	55	74	56	100%
AFM	48	55	61	56	
SAXS	53	61	70	54	
SEM	45	58	71		

- A second more complicated stack is analyzed here.
- This sample required floating one layer thickness and two layer optical constants as well as top, middle, and bottom widths.

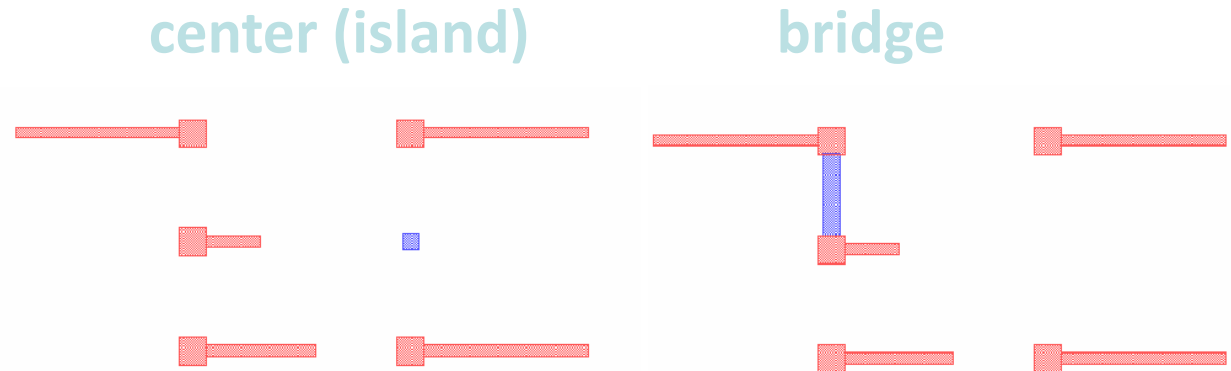
(2,6)

(3,6)

Defect Detection for Directional Patterning

32 nm Layout

R. Silver *et al.*, Proc.
SPIE 7638, 763802
(2010).



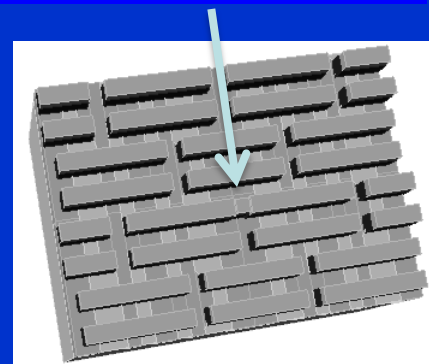
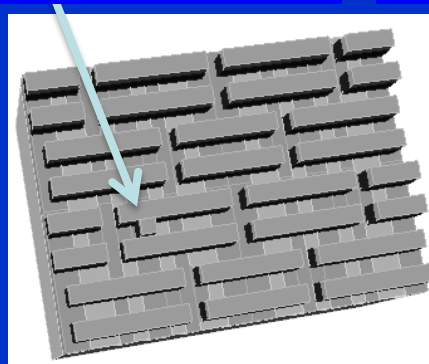
line-to-line

end-to-end

40 nm

30 nm

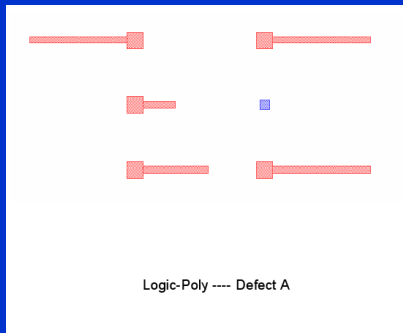
22 nm



T. Crimmins,
Proc. SPIE 7638,
76380H (2010).

Intentional defect array test structures to develop techniques.

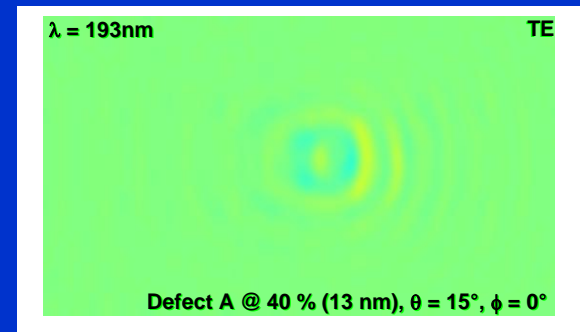
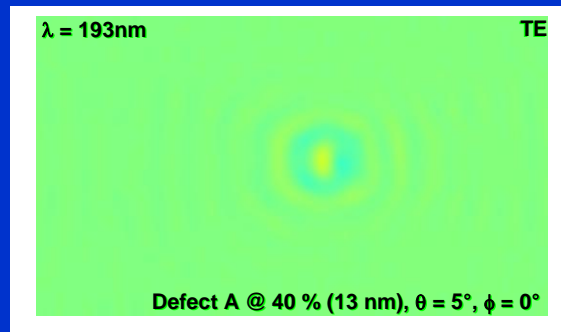
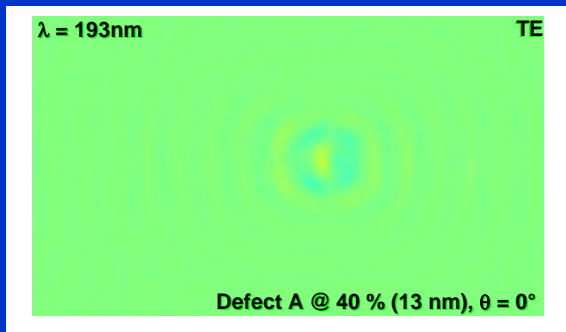
Defect A, Low Directionality



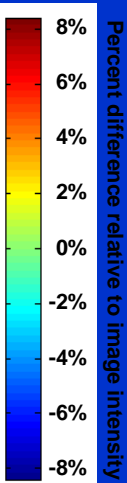
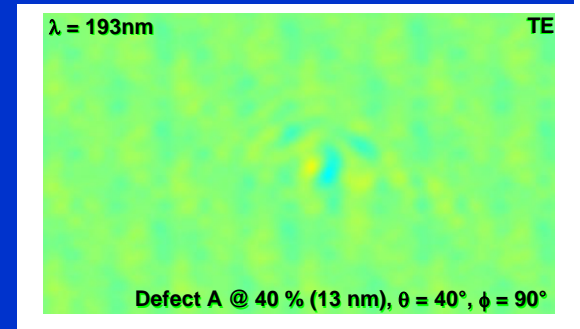
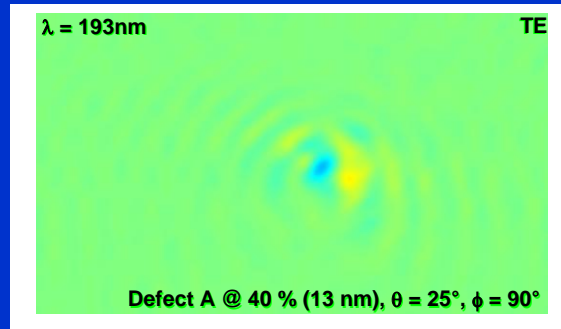
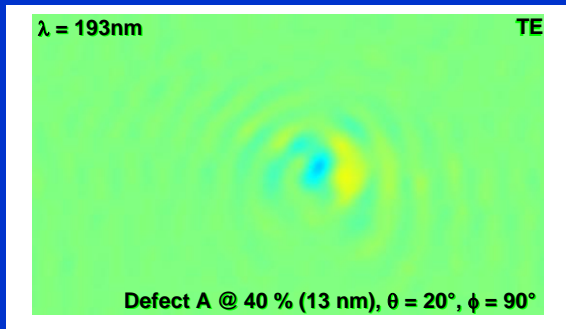
Defects A (Center) were modeled at several oblique angles.

FDTD (commercial) simulations

Fixed $\phi = 0$, TE Polarization



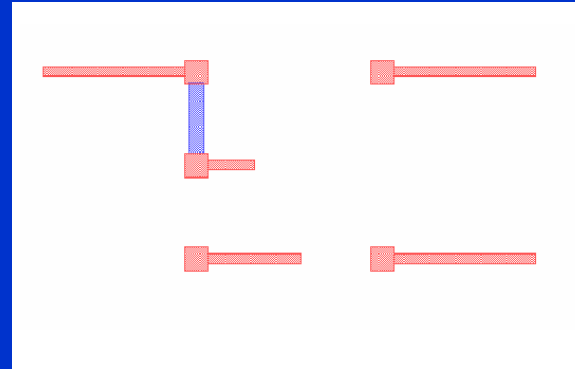
Fixed $\phi = 90$, TE Polarization



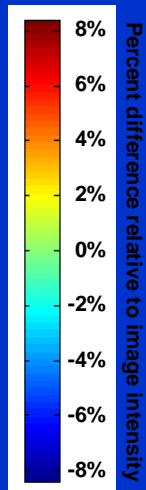
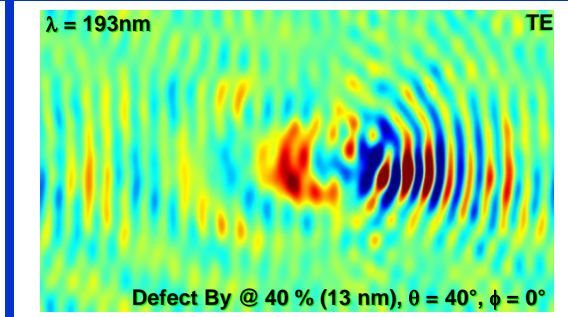
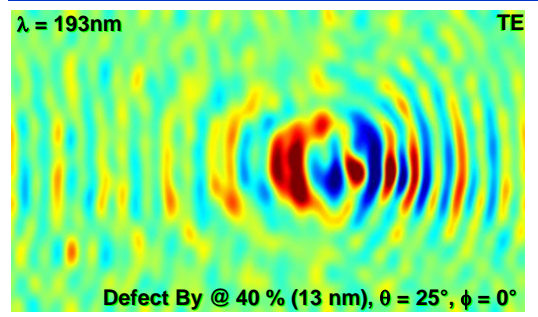
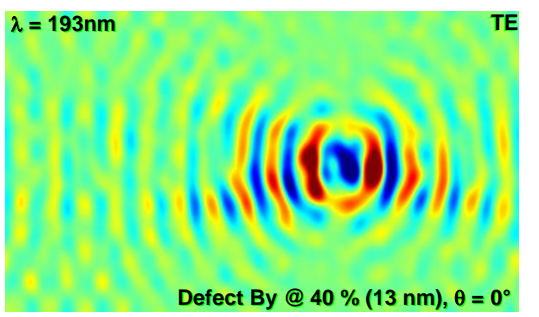
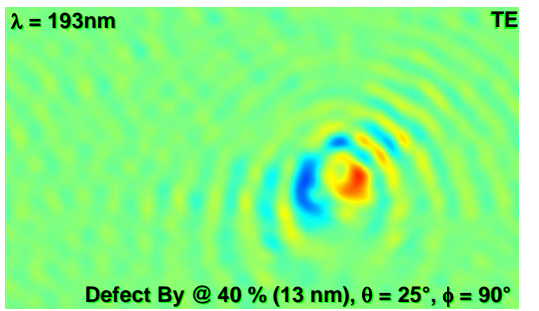
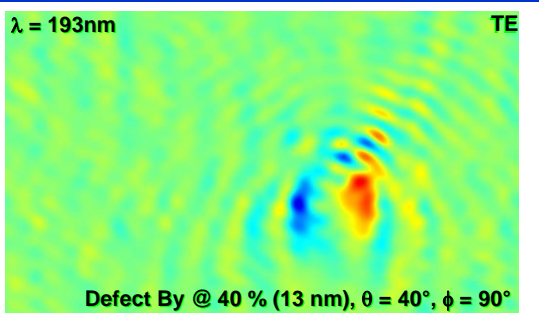
As θ increases, the ripples in the difference signal are shifting.

Defect By, High Directionality

FDTD (commercial)
simulations



Defects By (Bridge) were modeled at several oblique angles.

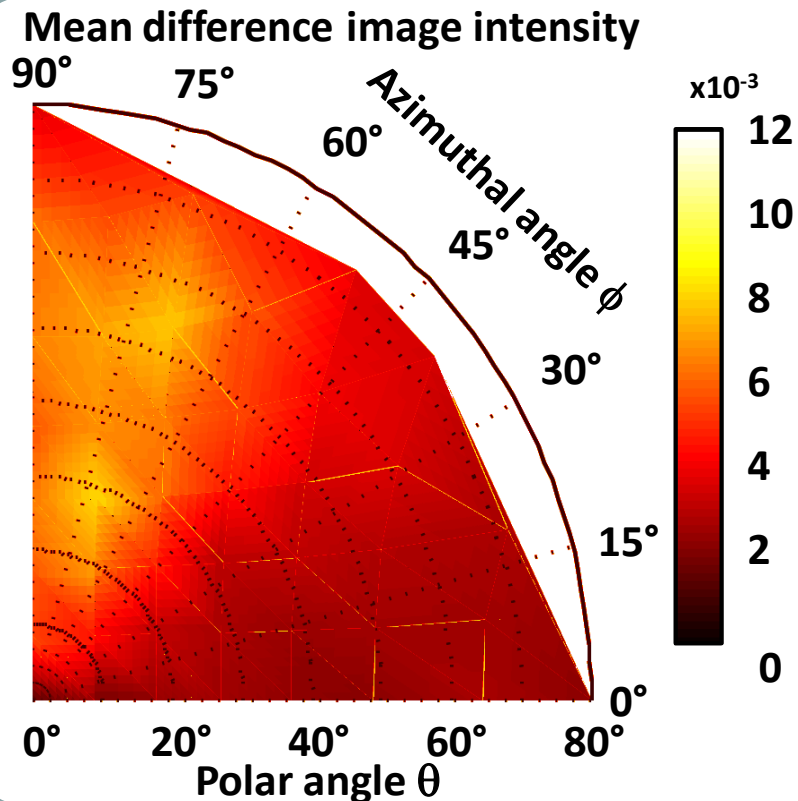


A clearly preferential incident direction is found.

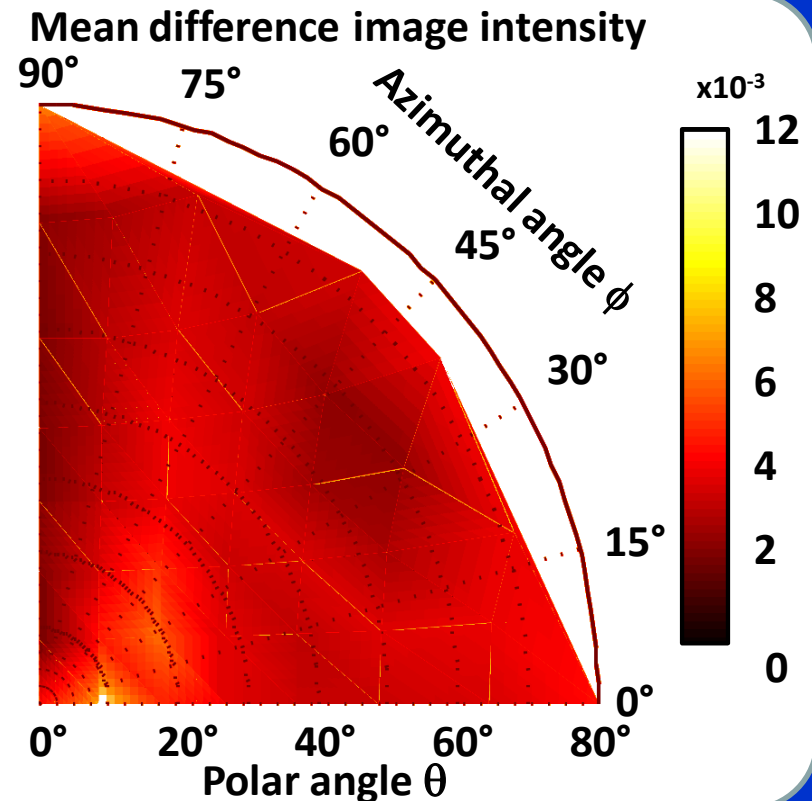
Polarization and angle for end-to-end

- High azimuthal angles with p polarization is best for detection.
- Low azimuth, p pol. and high azimuth, s pol. are both worse.

p polarization



s polarization

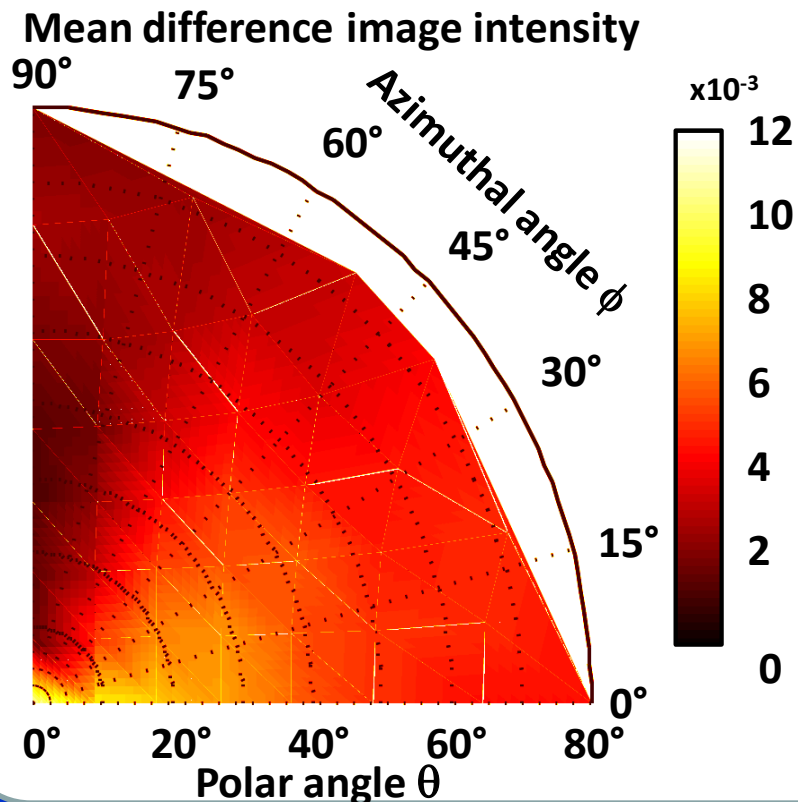


FEM simulation -- $\lambda=193$ nm -- 40 nm

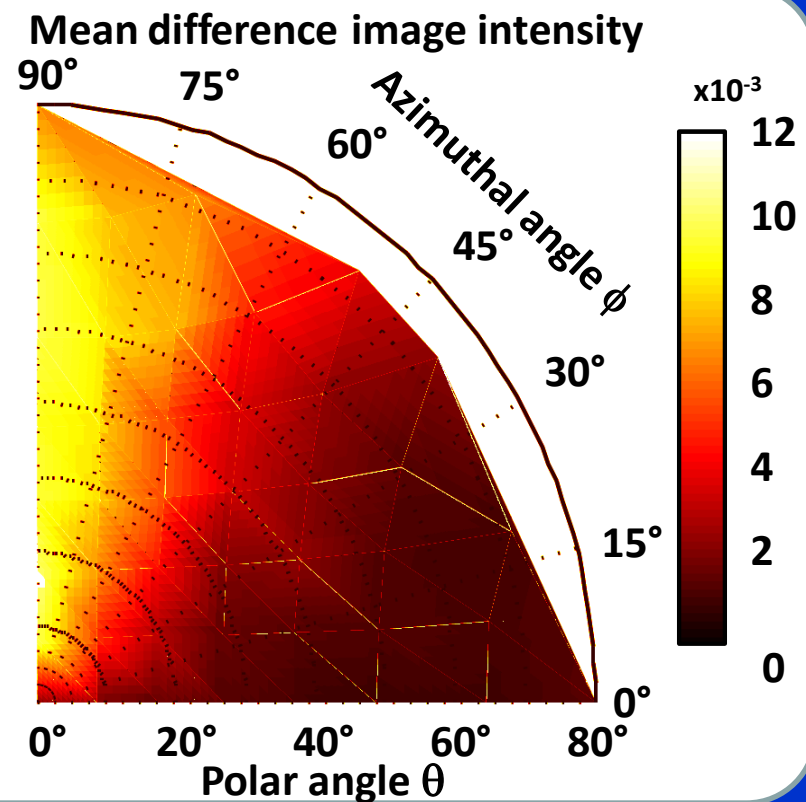
Polarization and angle for line-to-line

- High azimuthal angles with s polarization is best for detection.
- Line-to-line defect is orthogonal to the end-to-end defect.
- Defect detectability maps below show this orthogonality.

p polarization

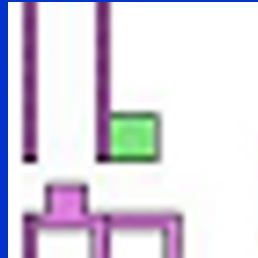


s polarization

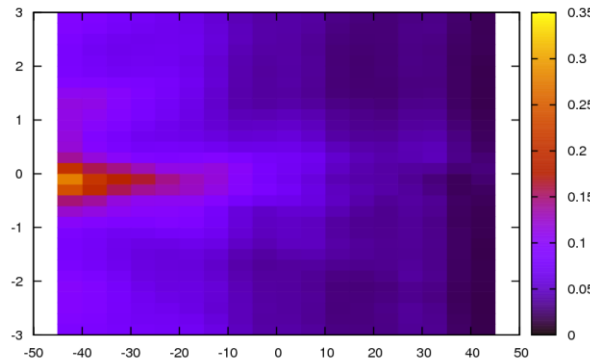


Wavelength Comparison: Simulation Study

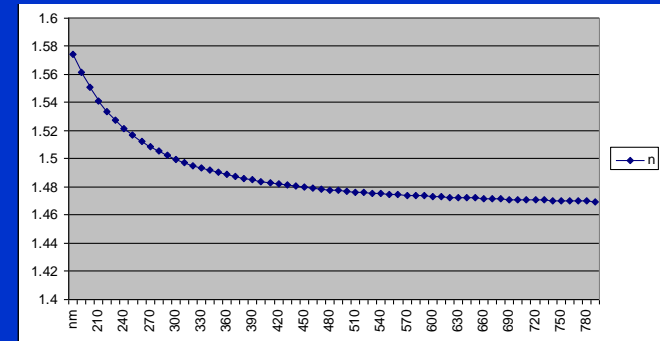
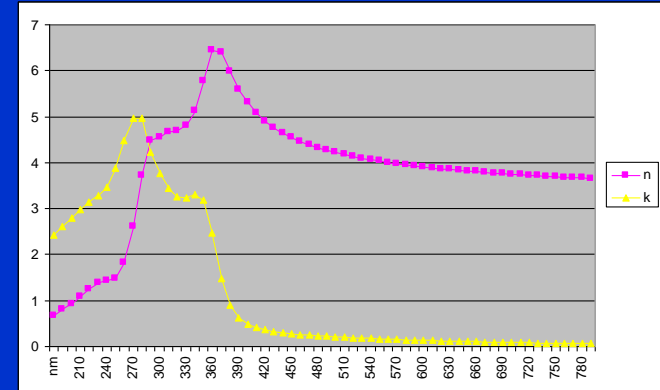
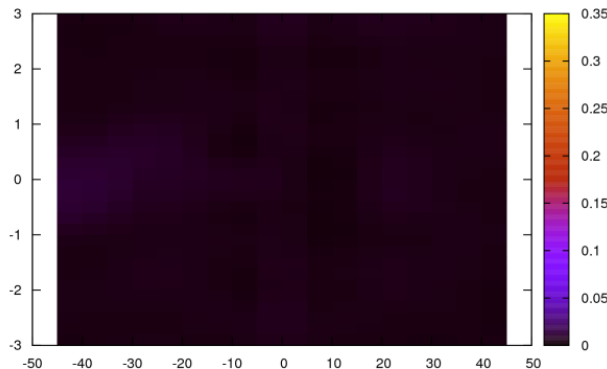
Defect Cx
Line Extension



Cx40
193nm
Ph = 0



Cx40
546nm
Ph = 0

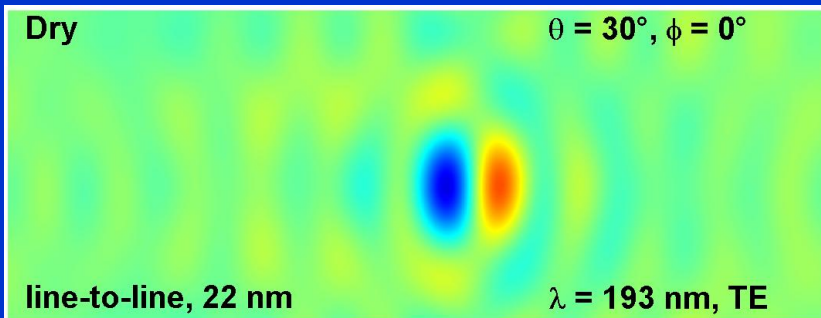
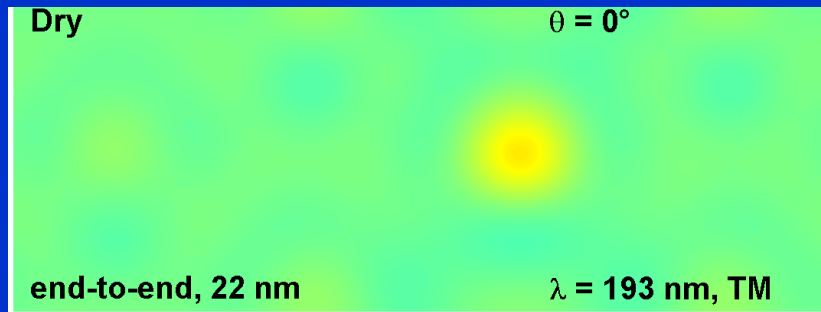


- Figures on the left are differential images at the wavelengths as labeled.
- The upper figure shows optical constants, n and k, for polysilicon and optical constants, n and k=0 for TEOS as used in the metal stack.

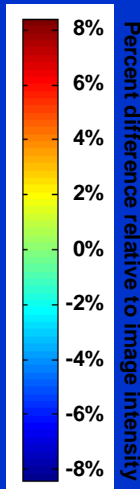
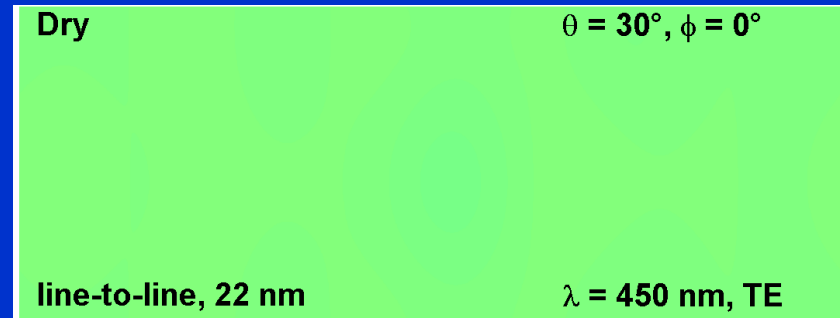
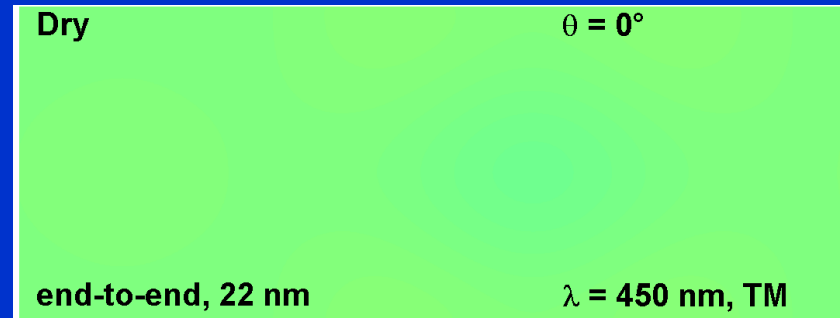
40 nm defect target

Wavelength Comparison

$\lambda = 193$ nm



$\lambda = 450$ nm

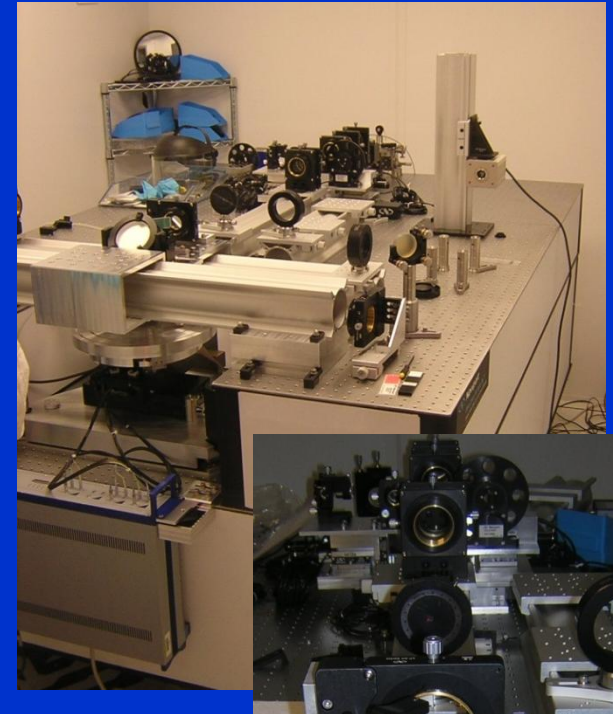
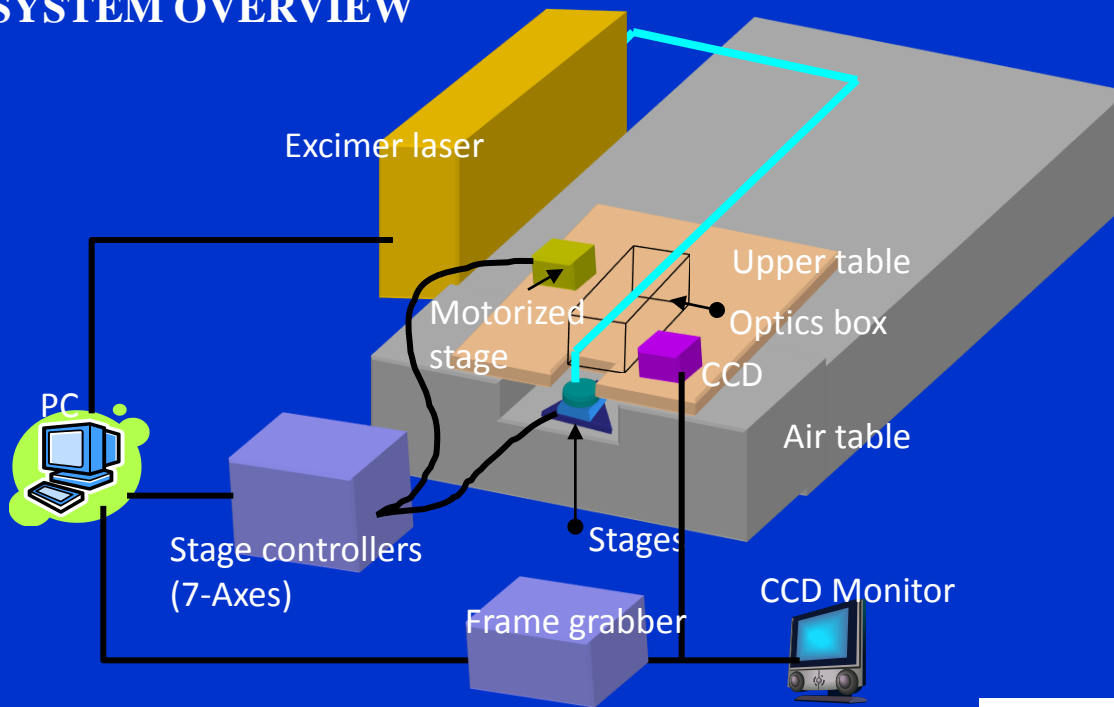


Defects with dimensions of $d < \lambda/20$ do not appear in the difference images.

22 nm node target
FDTD (commercial)
simulations

193 nm Excimer Laser Optical Metrology System

SYSTEM OVERVIEW



Angular Scan Mode

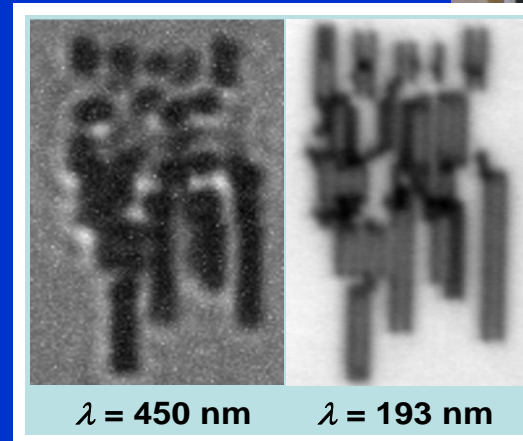
- Nearly plane wave illumination
- Pinhole apertures 20 μm ~200 μm
- Control of illumination angle, polarization, and phase

Full Field Modification Mode

- Modify distribution of illumination
- Motorized rotating aperture holder
- Modify spatial intensity distribution
- Control polarization state



Fourier image of dipole illumination



$\lambda = 450 \text{ nm}$

$\lambda = 193 \text{ nm}$

$\lambda = 193$ nm, varying illumination numerical aperture

Unpolarized, inner INA = 0.11

INA: 0.74

INA:
0.55

INA: 0.43

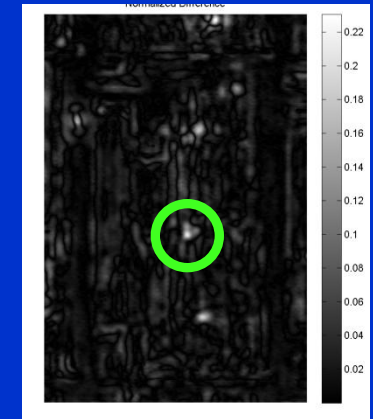
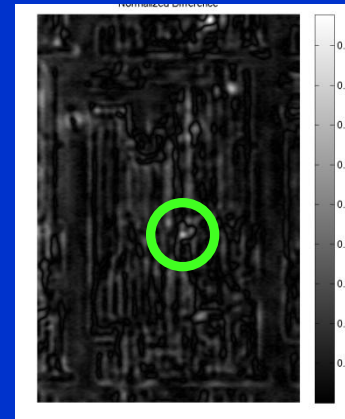
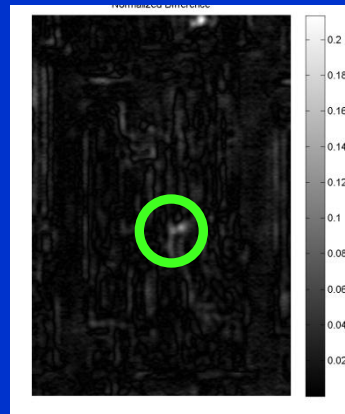
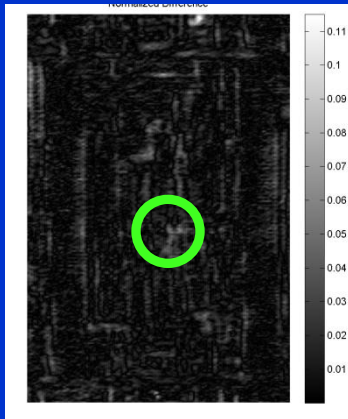
INA: 0.37

$\theta = 6^\circ$ to 47°

$\theta = 6^\circ$ to 33°

$\theta = 6^\circ$ to 25°


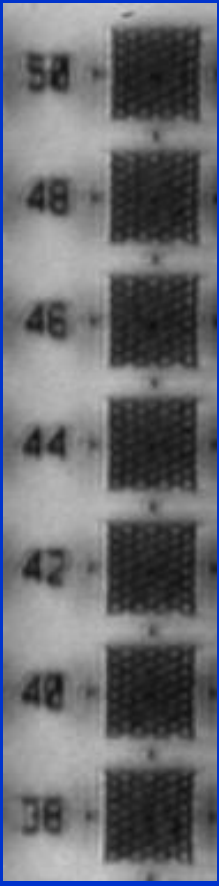
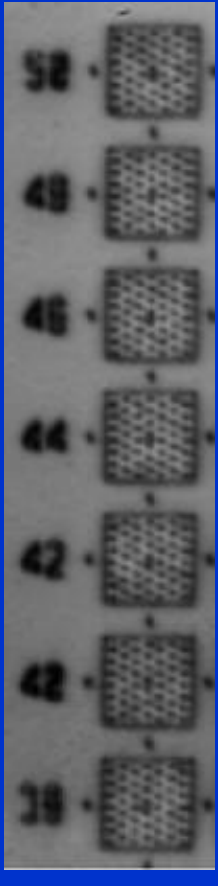
$\theta = 6^\circ$ to 22°



Defect size from SEM ~ 20 nm

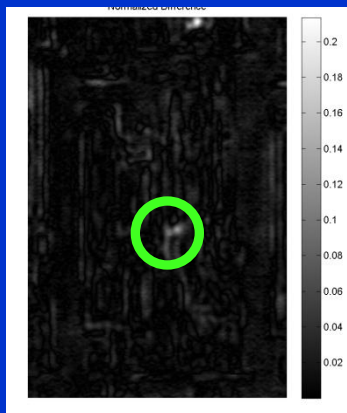
SEMATECH 65 nm Intentional
Defect Array wafer. Design rule,
25%

$\lambda = 193$ nm measurement of 30 nm targets

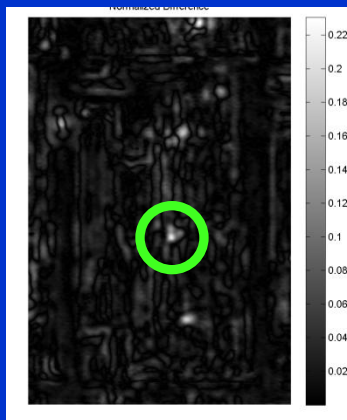
unpolarized		$\varphi=45^\circ$
Full-field illumination	Horizontally oriented dipole illumination	Full-field illumination
		

$\lambda = 193$ nm measurement of 20 nm and 30 nm targets

$\theta = 6^\circ$ to 33°



$\theta = 6^\circ$ to 22°



20 nm defects

unpolarized

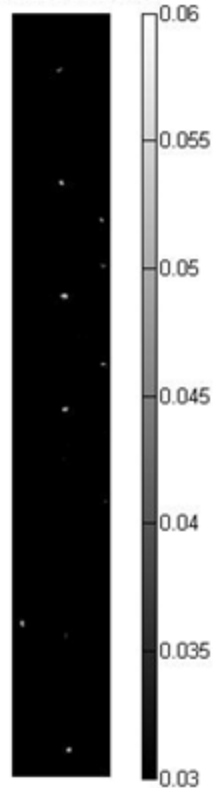
Full-field illumination

Horizontally oriented dipole illumination

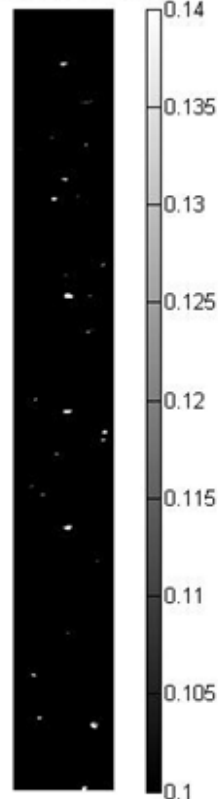
$\phi = 45^\circ$

Full-field illumination

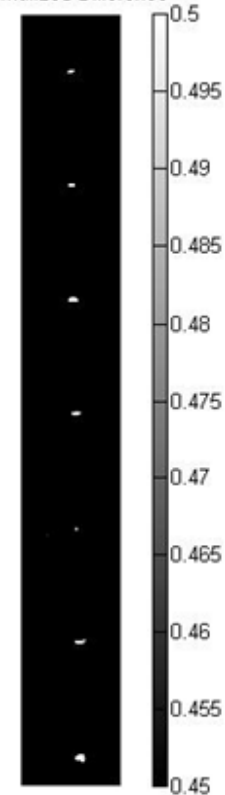
Normalized Difference



Normalized Difference



Normalized Difference

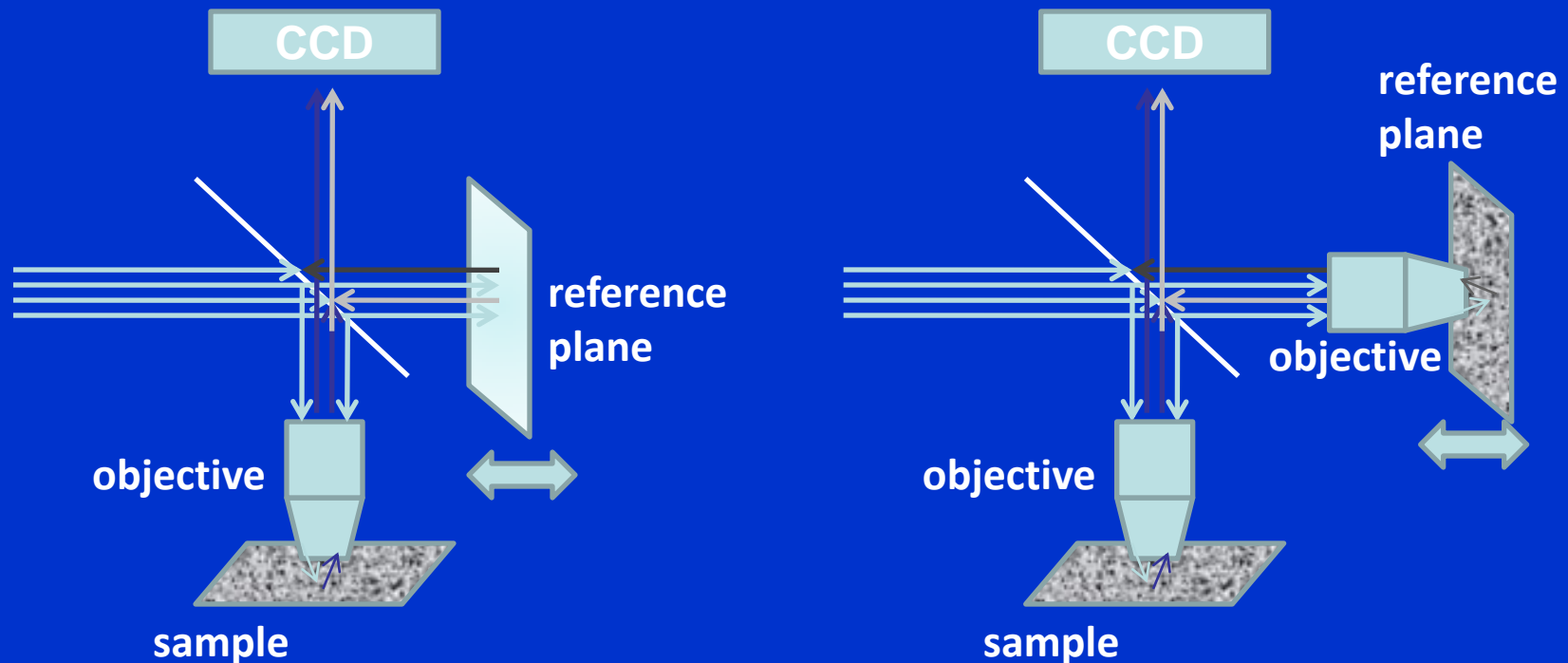


Gains from Coherent Imaging

- Introducing coherent illumination has several potential advantages, however this significantly complicates optical design

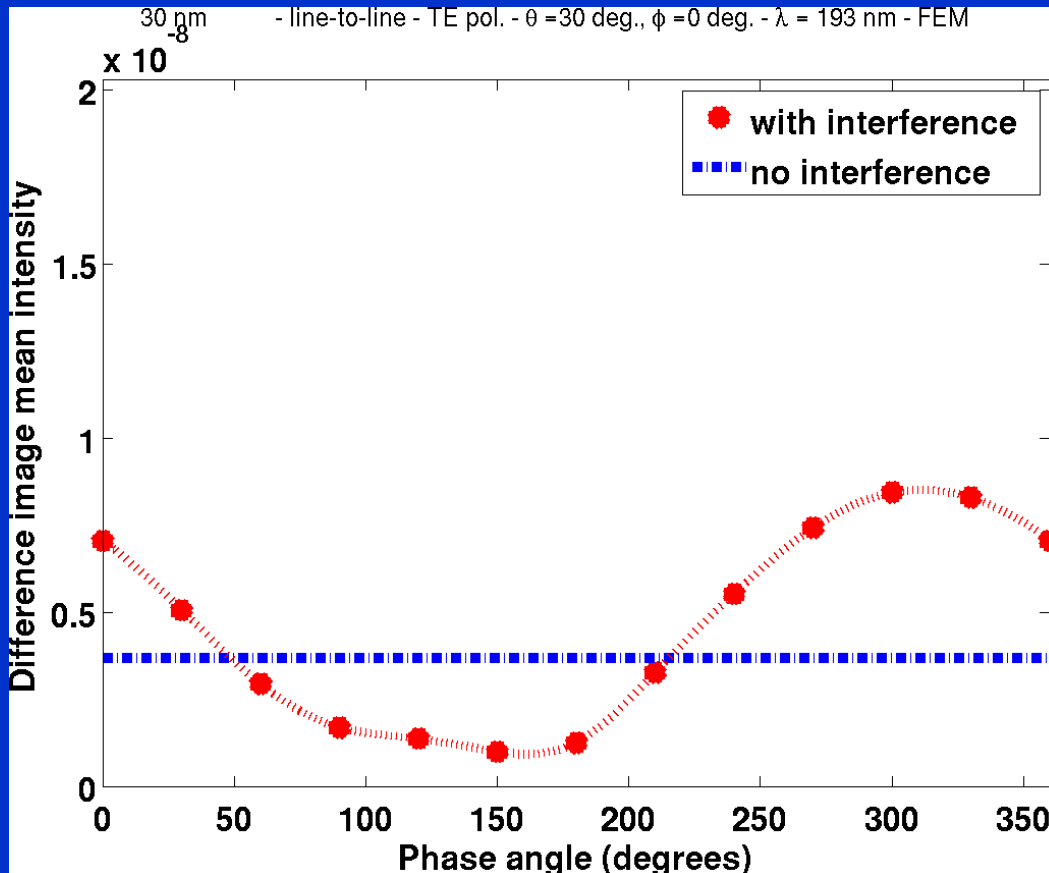
Interference Microscopy

Phase angle between the reference beam and the reflected beam is varied from 0 to 360 to improve detectability.



Interference Microscopy

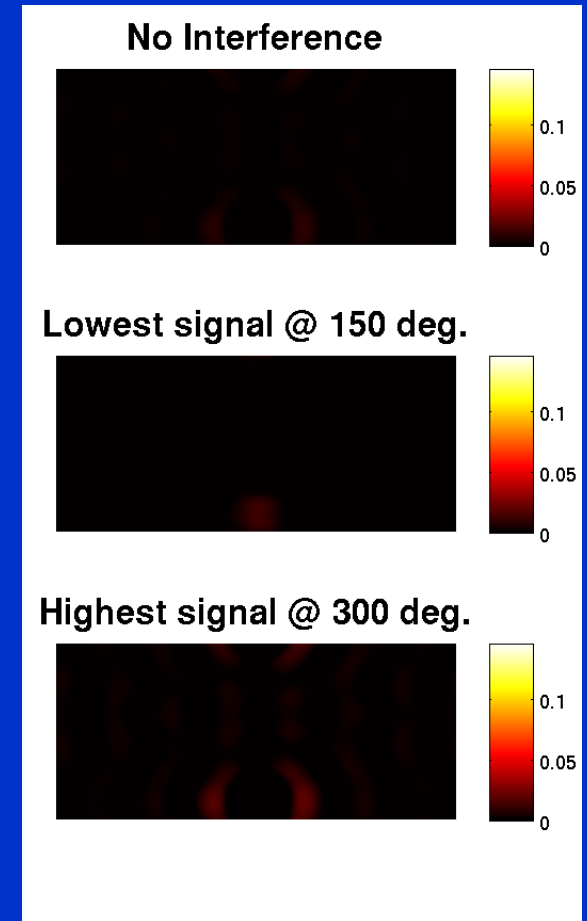
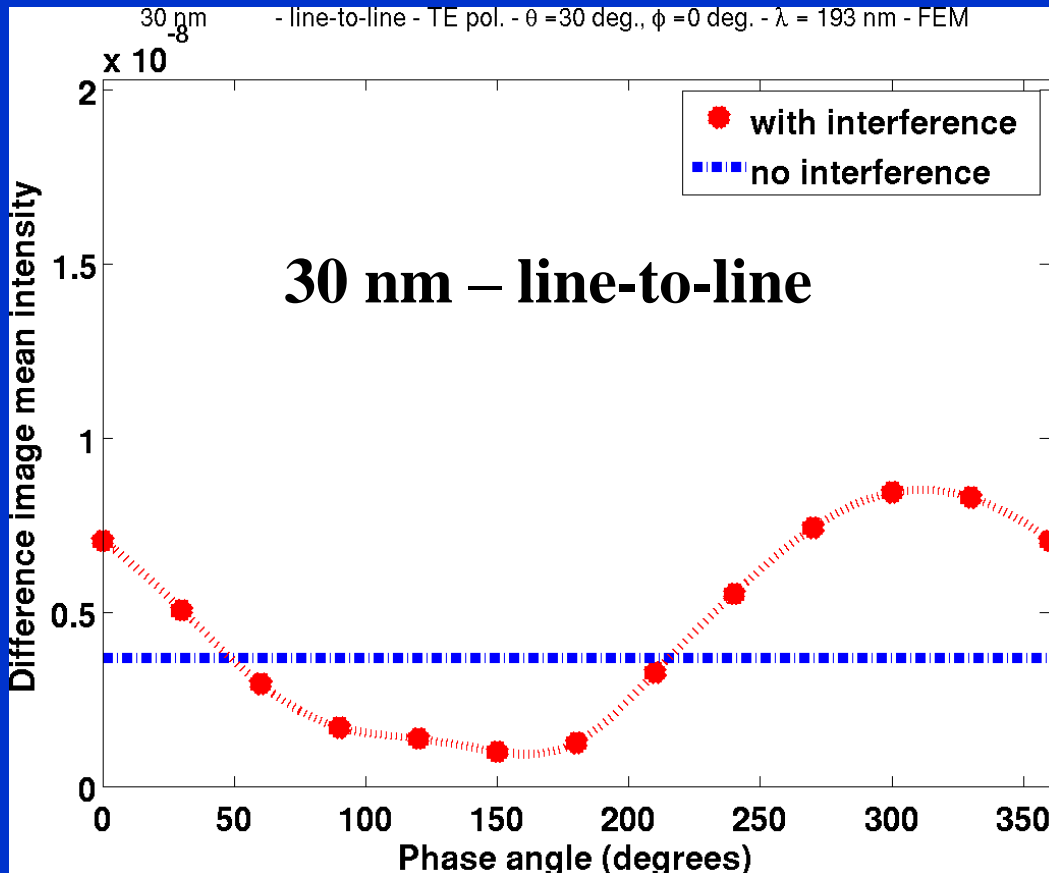
Simulated interference microscopy difference images have been calculated using the FEM model for 22nm, 30 nm, and 40 nm CD.



- The figure-of-merit is the mean per pixel of the absolute value of the difference image.
- The blue line shows the FOM without interference.
- The red line shows the shifting of the phase angle.

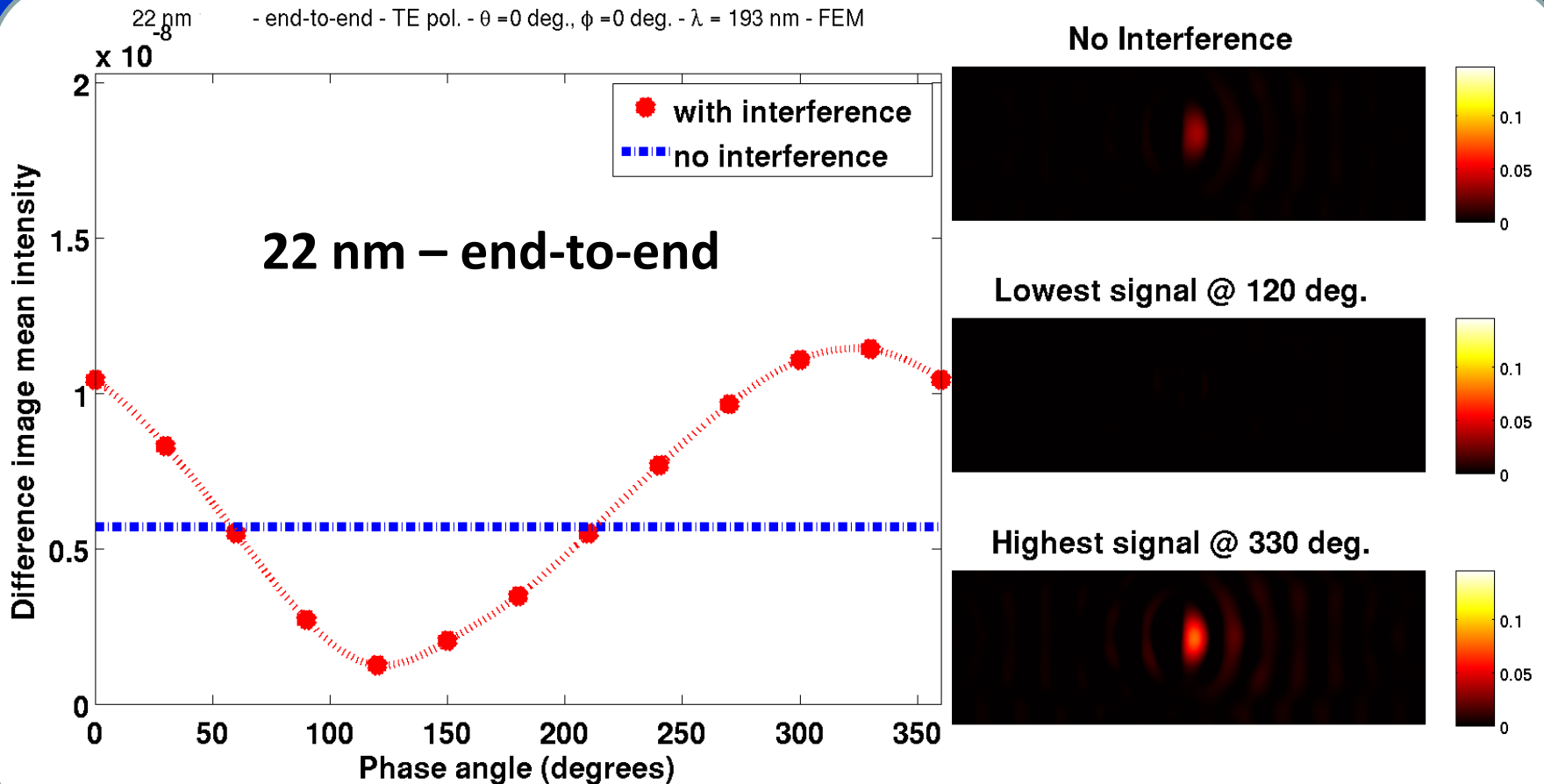
Interference Microscopy

Simulated interference microscopy difference images have been calculated using the FEM model for 22nm, 30 nm, and 40 nm CD.



Interference Microscopy

Interference microscopy using simple reference plane. Difference intensity images simulated using the FEM model for 22nm.



Future Directions

- **The directional aspects of future arrayed device fabrication are well suited to modulation of illumination and collection optical fields.**
- **Optical methods offer unparalleled throughput. Want to measure an entire wafer in an hour.**
- **Results clearly demonstrate gains operating at shorter wavelengths, no single optimum wavelength.**
- **Pulsed illumination has not been explored.**
- **Higher NA using immersion microscopy.**
- **New approaches in holographic/coherent differential imaging.**
- **Innovative new solutions are required to meet future high throughput defect metrology needs.**